

One-dimensional fermionic systems after interaction quenches and their description by bosonic field theories

Simone A. Hamerla^{1,*} and Götz S. Uhrig^{1,†}

¹*Lehrstuhl für Theoretische Physik I, Technische Universität Dortmund,
Otto-Hahn Straße 4, 44221 Dortmund, Germany*

(Dated: September 9, 2018)

We study the time evolution of two fermionic one-dimensional models (spinless fermions with nearest-neighbor repulsion and the Hubbard model) exposed to an interaction quench for short and moderate times. The method used to calculate the time dependence is a semi-numerical approach based on the Heisenberg equation of motion. We compare the results of this approach to results obtained by bosonization implying power law behavior. Indeed, we find that power laws describe our results well, but our results raise the issue which exponents occur. For spinless fermions it seems that the Tomonaga-Luttinger parameters work well which also describe the equilibrium low-energy physics. But for the Hubbard model this is not the case. Instead, we find that exponents from the bosonization around the initial state work well. Finally, we discuss what can be expected for the long-time behavior.

PACS numbers: 05.70.Ln, 71.10.Pm, 67.85.-d, 71.10.Fd

I. INTRODUCTION

Lately, the interest in nonequilibrium physics has risen significantly. This is due to the progress on the experimental side where many experimental setups have been developed which can be used to study many-body systems far from equilibrium. Amongst these setups are femtosecond photospectroscopy¹ and cold atomic gases trapped in optical lattices^{2,3}. Due to their excellent decoupling of the atoms from any environment the time evolution of atoms in optical lattices can be viewed as realizations of closed quantum systems. The relevant issues comprise the temporal evolution on short, on intermediate and on long time scales. In the present article, we focus on short and intermediate time scales.

Since these systems usually are in highly excited states involving many degrees of freedom developing quickly already on short time scales, a theoretical description is very challenging and requires new theoretical approaches. In the last years, techniques have been developed to deal with systems out of equilibrium. Amongst these are DMFT techniques^{4–6}, time dependent DMRG^{7,8}, light-cone renormalization⁹, methods based on CUT techniques¹⁰, on variational approaches including mean-field theories^{11–13}, on perturbative renormalization of Keldysh Green functions¹⁴, and on QMC techniques¹⁵, for a review see Ref. 16.

There are several ways to realize states far from equilibrium. A widely considered scenario are quenches, i.e., sudden changes in the intrinsic system parameters¹⁷. In this work we focus on interaction quenches, where the interaction H_{int} is abruptly changed^{10,11,14,15,18–22}. We will focus on quenches where the interaction is switched from zero to a finite value. Thus, the system is prepared initially in the ground state of a non-interacting Hamiltonian H_0 . But the time evolution is governed by the interacting Hamiltonian $H = H_0 + H_{\text{int}}$. In this way, the

system is in a highly excited state with respect to H .

In the present work, we study the time evolution of two generic fermionic lattice models in one dimension (1D). Of course, bosonic models are investigated in other studies as well^{12,13,19,23–27}. One-dimensional models play a special role in the context of thermalization because in these models an exhaustive number of conserved quantities may exist. Naturally, the existence of conserved quantities influences the dynamics of the system strongly²⁸. The first model to be studied are spinless fermions with nearest-neighbor repulsion. The quench dynamics of this system is contrasted to the quench dynamics of the second model, the one-dimensional Hubbard model which includes the spin degree of freedom. Both models are integrable.

In equilibrium, one-dimensional models are tackled by many analytical and numerical methods whose review is far beyond the scope of the present article. For the purposes of the present article, it is sufficient to note that gapless one-dimensional models with linear dispersion at low energies can be efficiently described by bosonic field theories^{29–35}. Often, the bosonic fields can be taken to be without interactions at low energies. For instance, this is the case for spinless fermions. For models including spin, sine-Gordon models include the leading bosonic interaction^{33,35}. Naturally, the question arises whether the same or similar bosonic field theories are also able to describe the nonequilibrium dynamics^{36–38}. Quenches of the non-interacting bosonic models are fairly well understood by now^{18,21,39,40}. A set of results for the sine-Gordon model is also available^{14,23–26,41}.

The quenches considered in this work start from non-interacting Fermi seas. For these initial states the momentum distribution displays a jump at the Fermi points at $\pm k_F$, where the occupation drops from unity to zero on passing from $|k| < k_F$ to $|k| > k_F$. Exposed to the quench, the jump in the momentum distribution of the system evolves in time which provides a sensitive probe

for the quench dynamics.

We calculate the time evolution of the jump in the momentum distribution by a semi-numerical approach based on the Heisenberg equations of motion. The method is used to investigate the behavior of the two models on short and intermediate times after the quench. Here we focus on the non-oscillatory, smooth decay of the jump; thus we study not too strong quenches which remain in the metallic regime. The oscillatory behavior occurring for strong quenches into insulating phases or close to them was studied separately⁴² for the sake of clarity⁴³. For the accessible times, the dynamics of the jump can be described by the non-interacting bosonic field theories. But we find evidence that the underlying parameters differ from their values at equilibrium. We discuss various scenarios for the behavior at longer times.

The paper is organized as follows. In the next section, the models under study are presented and the semi-numerical method used to calculate the time dependence of the jump is explained, and the expectations from bosonic field theories are recalled. In section III, results for the spinless fermion model and for the Hubbard model are shown and compared to the field theoretic expectations. Section IV discusses the long-time behavior. In the last section, the results are summarized.

II. MODELS AND METHODS

A. Models

The first model under study are spinless fermions

$$H_{\text{NN}} = -J \sum_{\langle i,j \rangle} (\hat{c}_i^\dagger \hat{c}_j + \text{h.c.}) + U(t) \sum_i \hat{n}_i \hat{n}_{i+1} \quad (1)$$

with nearest-neighbor repulsion (NN). The operator \hat{c}_j^\dagger (\hat{c}_j) creates (annihilates) a particle at site j and $\hat{n}_j = \hat{c}_j^\dagger \hat{c}_j$. By a Jordan-Wigner transformation it can be mapped to an anisotropic spin $S = 1/2$ XXZ chain⁴⁵. It is integrable by Bethe ansatz^{46,47}.

The second model is the Hubbard model⁴⁸⁻⁵⁰ comprising spin $\sigma = \uparrow, \downarrow$

$$H_{\text{Hu}} = -J \sum_{\langle i,j; \sigma \rangle} (\hat{c}_{i,\sigma}^\dagger \hat{c}_{j,\sigma} + \text{h.c.}) + U(t) \sum_i \hat{n}_{i,\uparrow} \hat{n}_{i,\downarrow} \quad (2)$$

which is governed by the hopping J and the local repulsion U . This model as well is exactly solvable by Bethe ansatz^{51,52}.

We focus on quenches where the interaction is switched on $U(t) = \Theta(t)U \geq 0$ abruptly and consider Fermi seas as initial states, i.e., the ground states for $U = 0$. Throughout, the band width $W = 4J$ is used as natural energy scale and consequently time is measured in the inverse band width $1/W$ since we set \hbar to unity.

B. Methods

Below some quantities with spin σ are denoted for the Hubbard model. In the corresponding quantities without spin, i.e., for the spinless fermion model, the subscript σ is to be omitted.

For $U = 0$, the momentum distribution shows a jump at the Fermi momentum $k = k_F$. Under the influence of the quench the jump

$$\Delta_n(t) = \lim_{k \rightarrow k_F^+} n_{k,\sigma}(t) - \lim_{k \rightarrow k_F^-} n_{k,\sigma}(t) \quad (3)$$

is reduced.

The momentum distribution of the system can be calculated by the Fourier transformation of the one-particle correlation function

$$G_\sigma(\vec{r}, t) = \langle 0 | \hat{c}_\sigma(\vec{r}, t) \hat{c}_\sigma(0, t)^\dagger | 0 \rangle \quad (4)$$

where the expectation value is taken with respect to the non-interacting Fermi sea $|0\rangle$. Thus the time dependence of the operators \hat{c}_σ and \hat{c}_σ^\dagger is needed.

To capture the time evolution of these operators we use the the following ansatz²¹

$$\hat{c}_\sigma^\dagger(\vec{r}, t) = \hat{T}_{\vec{r}}^\dagger + \hat{T}_{\vec{r}}^\dagger \left(\hat{T}^\dagger \hat{L}^\dagger \right)_{\vec{r}} + \dots \quad (5)$$

with \hat{T}^\dagger (\hat{L}^\dagger) denoting a general superposition of particle (hole) creation operators. For instance \hat{T}^\dagger is given by

$$\hat{T}_{\vec{r}}^\dagger = \sum_{|\vec{\delta}| \lesssim v_{\text{max}} t} \sum_\sigma h_0(\vec{\delta}, t) \hat{c}_{\vec{r} + \vec{\delta}, \sigma}^\dagger, \quad (6)$$

where the creation operators acting on site $\vec{r} + \vec{\delta}$ are summed weighted with the prefactor $h_0(\vec{\delta}, t)$. The shifts $\vec{\delta}$ are roughly bounded by the distance over which quasi-particles can move in the time t which is given by $v_{\text{max}} t$. This is the light-cone effect⁵³ first derived by Lieb and Robinson⁵⁴. The effect of correlations beyond this bound is exponentially small. The more complex terms $\hat{T}_{\vec{r}}^\dagger \left(\hat{T}^\dagger \hat{L}^\dagger \right)_{\vec{r}}$ are given by the superpositions of two creation and one annihilation operator. Another particle-hole pair $\hat{T}^\dagger \hat{L}^\dagger$ adds another creation and annihilation operator and so on.

The prefactors $h(\vec{\delta}, t)$ contain the whole time dependence of the operators $\hat{T}_{\vec{r}}^\dagger$ and $\hat{L}_{\vec{r}}^\dagger$ and thus they determine the time dependence of $\hat{c}^\dagger(\vec{r}, t)$. To calculate the time dependence of the prefactors we use the equation of motion

$$\partial_t \hat{A}(\vec{r}, t) = i \left[\hat{H}, \hat{A}(\vec{r}, t) \right] \quad (7)$$

for the time derivative of any operator \hat{A} . The advantage of dealing with the time dependence for the operators instead of the one for the quantum states is the dependence

on the size of the system. For dealing with time dependent states we would be obliged to treat states in an infinite quantum system which is very difficult. In contrast, the appearance of the commutators in the time dependence of the operators implies a linked-cluster property. In other words, up to a certain order m in the time t one has to deal only with a finite number of operators while dealing with the infinite system in the thermodynamic limit. We stress that all results presented here refer to this limit. The caveat of the approach is that the number of operators grows exponentially with the order m .

When calculating the commutator $[\hat{H}, \hat{c}^\dagger(\vec{r}, t)]$ we encounter two cases. (i) The commutation with the non-interacting part of the Hamiltonian \hat{H}_0 leads to a shift of single fermionic operators. (ii) The commutation with the interaction term \hat{H}_{int} creates or annihilates additional particle-hole pairs $(\hat{T}^\dagger \hat{L}^\dagger)$. Iterating the commutation leads to the ansatz (5) and extends it step by step. Each commutation creates more and more terms with higher and higher number of particles and holes involved.

Comparing the coefficients of the left hand side and of the right hand side of the Heisenberg equation (7) yields differential equations for the prefactors h . Then, this set of differential equations is solved numerically. The initial conditions of the prefactors are $h_0(0, 0) = 1$ and $h_i(\vec{r}, t) = 0 \forall i \neq 0$.

Since each commutation adds the coefficients necessary to describe another order in time t the results become more and more accurate on increasing number of commutations (loops). In this way a calculation with n commutations provides results for $\hat{c}^\dagger(t)$ which are exact up to order t^n . To quantify the convergence of the results calculations with different numbers of commutations are performed and compared. One may introduce a time t_{runaway} up to which the deviations between the results do not exceed a certain threshold, for instance 10^{-2} . Thus, the precise definition of t_{runaway} depends on the threshold, but for a given reasonable value of the threshold one can clearly see that the results become more and more accurate for increasing number of loops. This has been performed for results for the Hubbard model in Appendix A of Ref. 42 and results for the spinless fermions can be found in Appendix A below. The results in Appendix A of Ref. 42 and those in Appendix A below show that t_{runaway} increases roughly quadratically with the number of loops m , i.e., $t_{\text{runaway}} \propto m^2$

C. Bosonization Results

We briefly recall what is to be expected for the jump in the momentum distribution in Tomonaga-Luttinger models of non-interacting bosons^{18,21,39,40}.

For the spinless case one finds²¹

$$\Delta n(t) = \left[\frac{r^2}{r^2 + (2vt)^2} \right]^{2\gamma(1+\gamma)} \quad (8)$$

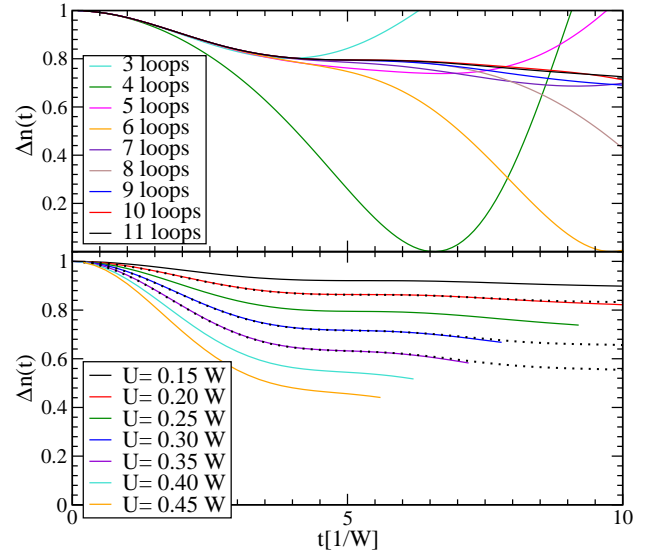


FIG. 1: (color online) Upper panel: Jump $\Delta n(t)$ in the half filled spinless fermions model for various loop numbers. Lower panel: $\Delta n(t)$ for increasing U (from top to bottom at small t) in 11 loops. The dotted lines display exemplary DMRG data from Karrasch et al.³⁶ illustrating the quantitative agreement in the range where our data is converged.

where v is the dressed velocity in the system and r the characteristic length scale of the interaction. The leading power law in time t without the length scale r in the denominator was first derived by Cazalilla¹⁸. In the above formula, the interaction is assumed to range over all momenta, i.e., from $-\infty$ to ∞ . If a finite range in momentum space is assumed oscillations occur. The occurrence of oscillations stemming from the high-energy cutoff is indeed generic^{23,40,53}. Note that such a finite range is natural in microscopic models because the finite extension of the Brillouin zone limits the range of the interaction space.

The exponent in (8) is determined by γ which is related to the standard bosonization parameter in the usual way

$$\gamma = (K + K^{-1} - 2)/4. \quad (9)$$

Note that the expression (8) is governed by an exponent related to the one occurring in equilibrium³¹ except that γ in equilibrium has been replaced by $2\gamma(1 + \gamma)$ after the quench²¹. Thus, for small values one finds a factor of 2, similar to the observation after quenches of other systems⁵⁵. We stress that the replacement $\gamma \rightarrow 2\gamma(1 + \gamma)$ is an inherent property of the Tomonaga-Luttinger model. It is not related to any underlying microscopic model.

In the presence of spin, the above formulae are modified. The Hamiltonian is given by the non-interacting sum of the spin part and of the charge part. Consequently, the single-particle correlation (4) and hence the jump are given by the product of the responses in the

spin and the charge channel²¹

$$\Delta n(t) = \left[\frac{r_\rho^2}{r_\rho^2 + (2v_\rho t)^2} \right]^{\gamma_\rho(1+\gamma_\rho)} \left[\frac{r_\sigma^2}{r_\sigma^2 + (2v_\sigma t)^2} \right]^{\gamma_\sigma(1+\gamma_\sigma)} \quad (10)$$

where $\nu \in \{\rho, \sigma\}$ stands for charge (ρ) or spin (σ) channel. Again, the parameters r_ν are the characteristic length scales of the interaction, v_ν the velocities and γ_ν the equilibrium exponents. The exponents can be expressed through the anomalous dimensions K_ν in the usual way

$$\gamma_\nu = (K_\nu + K_\nu^{-1} - 2)/4. \quad (11)$$

Note that the exponents in each channel separately take only half the value of their counterpart in the spinless case. This is again the same as in equilibrium^{31,33}. But also in the case with spin, the non-equilibrium exponents are obtained from the equilibrium ones by the replacement $\gamma_\nu \rightarrow 2\gamma_\nu(1 + \gamma_\nu)$.

III. RESULTS

A. Spinless Fermions

In this section, we present the results obtained by the equation of motion approach for the behavior of the spinless fermion model after the quench. We focus on short and intermediate times after the quench and show results for the jump $\Delta n(t)$. We explain the data from the equation of motion approach by comparing them to the bosonization results.

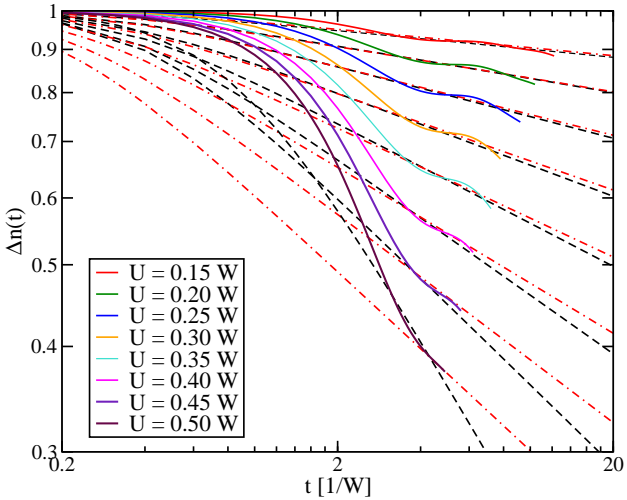


FIG. 2: (color online) Solid lines: $\Delta n(t)$ in the half filled model of spinless fermions for increasing U (from top to bottom) in 11 loops. Dashed (black) lines: $\Delta n(t)$ as in Eq. (8) with the ground state (GS) exponents from Eq. (12). Dashed-dotted (red) lines: $\Delta n(t)$ with the Fermi sea (FS) exponents from Eq. (14).

In Fig. 2 the jump $\Delta n(t)$ is shown for the spinless fermion model with nearest-neighbor repulsion. The data agrees very well with the data by Karrasch et al. in Fig. 1 of Ref. 36 obtained by time dependent infinite-size DMRG, for exemplary comparisons see Fig. 1.

First, we compare the data to the power law behavior (8). This still leaves the question which parameters are to be used. Certainly, a first trial are the parameters which describe the models in equilibrium. Since we are dealing with the systems at zero temperature the ‘equilibrium’ refers to the ground state and its immediate vicinity, i.e., the elementary excitations. Then, the anomalous dimension K and the velocity can be determined by Bethe ansatz^{29,47}. They read

$$K_{\text{GS}} = \pi/[2(\pi - \arccos(2U/W))] \quad (12a)$$

$$v_{\text{GS}} = \pi \sin(\arccos(2U/W))/[2 \arccos(2U/W)], \quad (12b)$$

where we use the subscript GS for ‘ground state’ to emphasize that these parameters pertain to the behavior of the model at the lowest energies in the vicinity of the ground state. The cutoff length r of the curves is fitted and evolves from 0.2 to 0.6 on increasing U , assuming that the lattice constant is set to unity. The formulae (12) are reasonable only up to $U = W/2$ where the system enters a gapped phase. The resulting anomalous dimension K is depicted in the left panel of Fig. 3 as dashed curve.

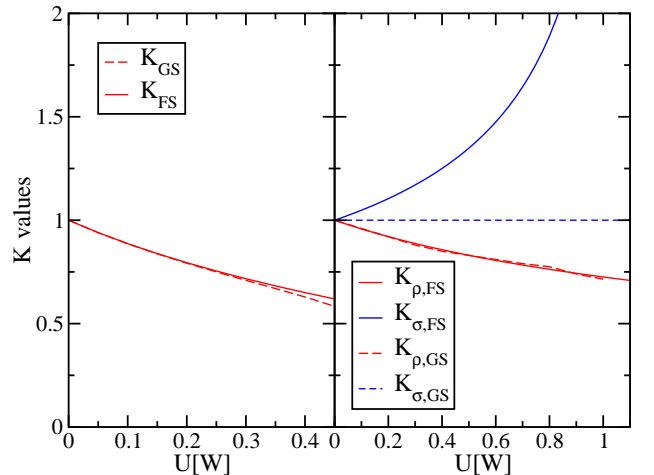


FIG. 3: (color online) Results for the anomalous dimensions $K_\nu, \nu \in \{\rho, \sigma\}$ obtained by bosonization. Dashed lines: Results obtained by bosonization around the ground state (GS) based on Bethe ansatz. Solid lines: K_ν values obtained by bosonization around the Fermi sea (FS). Left panel: Results for the spinless fermion model with nearest-neighbor repulsion. Right panel: Results for the Hubbard chain at quarter-filling; the Bethe ansatz is difficult to evaluate so that slight inaccuracies imply some minor wiggling of the dashed curve for K_ρ .

Inspecting Fig. 2 we see that the microscopic model displays oscillations in $\Delta n(t)$ which are absent in Eq. (8).

These oscillations are to be ascribed to the momentum cutoff of the interaction in microscopic models^{23,40,53}. Otherwise, the power law (8) nicely describes the accessible dynamics, at least for not too large values of the interaction. This observation agrees with the one by Karrasch et al. in Ref. 36.

We point out, however, that the agreement deteriorates for larger values of the interaction, namely for $U = 0.45W$ and for $U = 0.5W$. Thus we pose the question whether the equilibrium exponent γ is still the relevant one for non-equilibrium situations. We stress that the answer to this question in an unconditioned ‘Yes’ for the Tomonaga-Luttinger model itself. But for any microscopic model or for any model containing boson-boson interaction such as for instance the sine-Gordon model the behavior in the vicinity of the ground state will in general be *different* from the behavior at higher energies. This means that if we stick to the description of the quench of a microscopic model in terms of an approximate field theoretic model it must be expected that the parameters of this approximate model depend on the initial conditions, for example the extent of the quench. In the renormalization description of the sine-Gordon model off equilibrium by Mitra and Giamarchi^{14,41} such a dependence of the anomalous dimension K on the initial condition has appeared explicitly, even though the quench considered by them is not the same as here because the sine term is switched on only adiabatically long time after the sudden quench.

In order to assess how far a quench puts the microscopic model away from equilibrium, i.e., from the ground state, we define the quench energy ΔE

$$\Delta E := \langle \text{FS} | H(t > 0) | \text{FS} \rangle - \langle \text{GS} | H(t > 0) | \text{GS} \rangle \quad (13)$$

where $|\text{FS}\rangle$ stands for the initial state which in our case is a Fermi sea while $|\text{GS}\rangle$ stands for the ground state of the Hamiltonian after the quench. Thus, ΔE as defined above measures the total excitation energy above the ground state induced by the quench. In Ref. 26, this quantity is called the heat. It is conserved since the energy in a closed constant quantum system is a conserved quantity. We stress that quenches in *imaginary* time³⁶ which obey $|t\rangle = \exp(-H\tau)|\text{FS}\rangle$ do not conserve ΔE and thus behave differently.

In Fig. 4, it is plotted for the two models under study as function of the quenched interaction. For the spinless fermion model we note the quenched energy remains fairly small $\lesssim 3 \cdot 10^{-3}W$ for quenches below the phase transition at $U = W/2$ ^{46,47}. Thus one may not be surprised that the ground state parameters (12) yield good agreement. In Ref. 36, it was concluded that the dynamics of interaction quenches is universally governed by the equilibrium exponents.

An alternative argument to reach the parameters for the relevant field theoretic model after a quench is the following. The dynamics after the quench starts from the initial state, here $|\text{FS}\rangle$. The short time dynamics implies the iterated gradual excitation of particle-hole

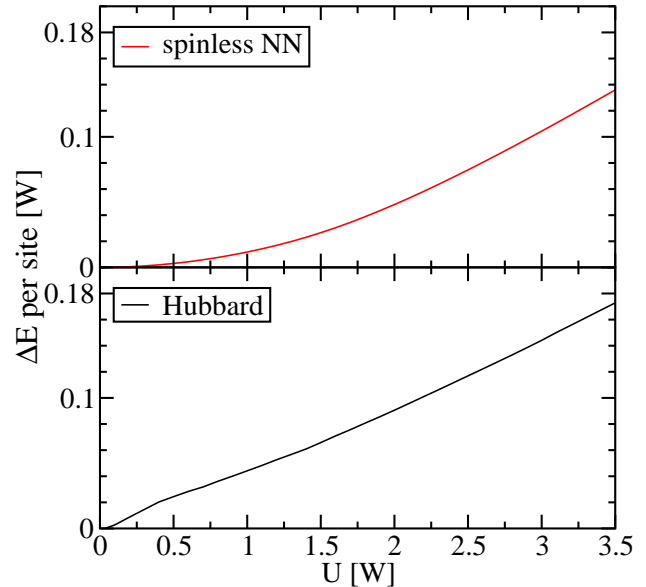


FIG. 4: (color online) Excitation energies ΔE per site defined in (13) in dependence on the interaction strength U for the spinless fermions model at half-filling (upper panel) and for the quarter-filled Hubbard model (lower panel); the behavior at low values of U is quadratic even though the difficult evaluation of the Bethe ansatz equations hindered us to reach very high precision. The results are very accurate at large U .

pairs²¹ so that up to moderate times only a limited number of particle-hole pairs need to be described. Thus bosonization of the density fluctuations around the initial states $|\text{FS}\rangle$ is expected to yield a valid description of the dynamics at short and intermediate times.

The bosonization in the vicinity of the Fermi sea (FS) corresponds to the bosonization in leading order in U because no feedback effects due to the interaction need to be included. This leads us to the expressions^{29,30,32–34}

$$K_{\text{FS}} = \sqrt{(\pi v_F - U)/(\pi v_F + 3U)} \quad (14a)$$

$$v_{\text{FS}} = (1/\pi) \sqrt{(\pi v_F + U)^2 - 4U^2}. \quad (14b)$$

The anomalous dimensions K are shown in the left panel of Fig. 3. The implied power laws for the jump Δn are included in Fig. 2 as dashed-dotted curves. The fitted cutoff length r varies from 0.2 to 0.1 on rising U .

Obviously, the difference between the curves from the GS and from the FS parameters is small, cf. Fig. 2. This can be understood easily in view of the small excitation energies ΔE . Nevertheless, we point out that for the largest interactions U the FS curves fit better to the numerical data than the GS curves. This underlines the relevance of the question which field theoretic model is the appropriate one off equilibrium.

We note that the bosonization in the vicinity of the Fermi sea leaves out certain effects that will become important at even stronger quenches, for instance the cur-

vature of the dispersion or the effect of higher order umklapp scattering. (At leading order in U , no umklapp scattering occurs for spinless fermions.) This restricts the validity of the FS formulae (14) to values of U below $\pi v_F \approx 1.57W$, where K_{FS} and v_{FS} vanish.

B. 1D Hubbard Model

Quenches in a model *with* spin are by themselves of great interest because such models are much closer to what is realized in strongly correlated systems such as Mott insulators. Moreover, they display dynamical transitions at half-filling if quenched strongly in infinite dimensions^{6,11} and in one dimension⁴².

In the present article, however, we focus on weaker quenches for fillings off half-filling. The reason is that we want to focus on models which are quenched within the metallic phase. Thus we focus on quarter-filling which also suppresses umklapp scattering, at least to leading order, so that a quench into a Mott insulating phase is avoided. Furthermore, the Hubbard model at quarter-filling displays two further interesting features.

The first is shown in the right panel of Fig. 3 where the anomalous dimensions in the charge and in the spin channel are depicted. The GS parameters are deduced from the ground state properties as obtained from Bethe ansatz^{52,56}. Note that $K_{\sigma,\text{GS}} = 1$ by spin rotational symmetry³⁵. The FS parameters are again those of the bosonization around the Fermi sea amounting up to the bosonization^{32,33} in leading order in the quenched interaction U

$$K_{\rho,\text{FS}} = \sqrt{2\pi v_F/(2\pi v_F + 2U)} \quad (15a)$$

$$K_{\sigma,\text{FS}} = \sqrt{2\pi v_F/(2\pi v_F - 2U)} \quad (15b)$$

$$v_{\rho,\text{FS}} = v_F \sqrt{1 + U/(\pi v_F)} \quad (15c)$$

$$v_{\sigma,\text{FS}} = v_F \sqrt{1 - U/(\pi v_F)}. \quad (15d)$$

The right panel of Fig. 3 shows that the charge dimensions agree surprisingly well in both calculations $K_{\rho,\text{GS}} \approx K_{\rho,\text{FS}}$. In contrast, the spin dimension $K_{\sigma,\text{GS}}$ and $K_{\sigma,\text{FS}}$ differ significantly. It is well known from the analysis of the renormalization of the underlying sine-Gordon model that $K_{\sigma,\text{GS}}$ converges to its final value only for exponentially small energy scales³⁵.

The second interesting aspect is the fact that in the Hubbard model a moderate interaction quench implies much larger excitation energies, see lower panel of Fig. 4. For instance, a quench to $U = 0.8W$ yields an excitation energy of about $0.036W$. Thus, in the Hubbard model we can more easily study the effects of a larger distance from the equilibrium situation.

The behavior of the system after strong quenches can be found in Ref. 42.

Fig. 5 shows the data for a quench to $U = 0.8W$ in the quarter-filled Hubbard model. The oscillations are again to be attributed to the finite momentum cutoff of the interaction in a lattice model.

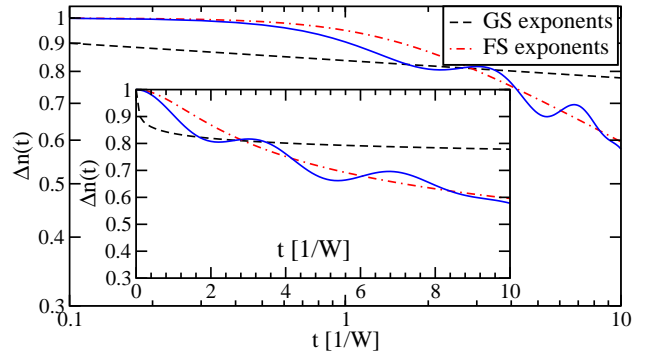


FIG. 5: (color online) Jump $\Delta n(t)$ for the Hubbard model at quarter-filling at $U = 0.8W$. Lines as in Fig. 2. For the GS exponents $r_\rho \approx 0.01$ is fitted; r_σ does not occur. For the FS exponents $r_\rho \approx 1$ and $r_\sigma \approx 0.6$ are fitted.

Inspecting the power laws, it is obvious that the GS and the FS power laws differ significantly as we expected from the significant differences in the anomalous dimensions and the significant excitation energy of the quench. We observe that the power law with the FS exponents fits much better than the power law with the GS exponents. As can be seen in the inset of Fig. 5, the GS exponents can only be used to describe the curve over a small range and the fitted range r_σ is unreasonably small.

We recall that even at equilibrium K_σ reaches its final (GS) value only for exponentially small energy scales ε . This implies that one must know the equal-time Green function at two points in space with exponentially large distance \vec{r} according to $\varepsilon \approx v_F/|\vec{r}|$ with the Fermi velocity v_F . After the quench, the correlations due to the switched interaction will develop gradually and spread out in time according to $|\vec{r}| \approx v_{\text{max}} t$, i.e., $1/t$ acts as a low-energy cutoff. Thus, effects at exponentially low energies are expected to show up only at exponentially large times if they are not superseded by other effects. For a discussion of the long-time behavior the reader is referred to the next section.

Here we state that the behavior at small and intermediate times is described better by the FS parameters (15). To support this finding, Fig. 6 shows the jump $\Delta n(t)$ for the Hubbard model at quarter-filling for various interaction strengths U . As can be seen in the upper panel, for small values $U \lesssim 0.3W$ the differences between the GS and the FS power laws are small so that they are indistinguishable on the accessible time scales.

For larger values of U , the time evolution of the jump is described very well by the FS power law while the GS exponents do not fit the slope of the decay of the jump towards larger times. Only the oscillations due to the high-energy cutoff^{23,40,53} are missed by the power law (10).

For larger $U \gtrsim W$ (lower panel) the agreement between microscopic data and the FS power laws deteriorates. We attribute this deterioration to the breakdown

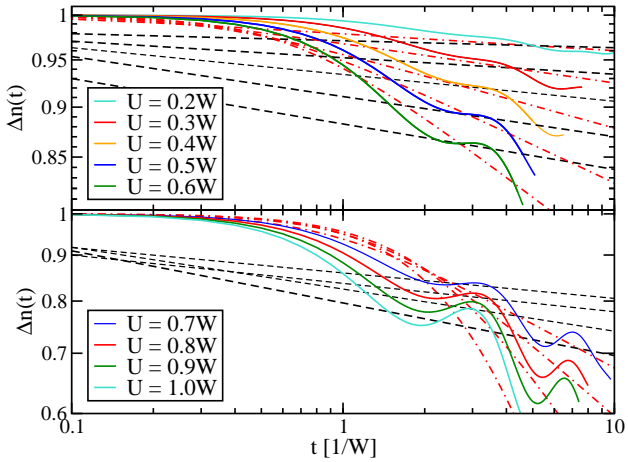


FIG. 6: (color online) Solid lines: $\Delta n(t)$ for the Hubbard model at quarter filling for various values of U . Dashed (black) lines: $\Delta n(t)$ given by the ground state (GS) exponents. Dashed-dotted (red) lines: $\Delta n(t)$ calculated with the Fermi sea (FS) exponents.

of the Tomonaga-Luttinger liquid description in terms of bosonic modes without interaction. Backscattering and the curvature of the single-particle dispersion are neglected. Hence for large excitation energies ΔE which take the system even further way from its equilibrium these effects need to be included. For short and intermediate times, however, they are of reduced relevance. For example, the leading correction due to backscattering is a term $\propto \int \cos(\sqrt{8}\Phi(x))dx$. But the expectation value of this and of any of its higher derivatives vanishes with respect to the Fermi sea because in the latter the fluctuations $\langle \Phi(x)^2 \rangle$ diverge which smears out the cosine term completely to zero, see also the discussion in Ref. 25.

IV. BEHAVIOR FOR LONGER TIMES

The next intriguing question is what happens for longer times t ? To date this question cannot be answered definitely. Numerically, no tools can treat *long* times far off equilibrium. Analytically, no general renormalization group theory for nonequilibrium physics exists. A study of the sine-Gordon model on the basis of Keldysh Green functions has been carried out^{14,41}. The non-interacting bosonic system is quenched at $t = 0$, but the sine term is switched on slowly afterwards. At present, it is unclear to which extent this calculation captures the scenario we are studying in the present article where the interaction is quenched abruptly at $t = 0$ in fermionic models.

To decide whether the results of the present article are relevant also for longer times we have to consider various energy cutoffs. The first was already mentioned above, namely the inverse time $\propto 1/t$. Given the accessible times, see Figs. 1, 2, and 6, we find that this cutoff is of order of about $0.1W$, the precise value depends on the

value of the interaction, the filling and the model under study. This is fairly large so that one may expect that the observed power laws will still gradually change for larger times.

But we come back to the distance of a quenched system to the true ground state which is measured by the excitation energy ΔE per site in (13), see Fig. 4. We anticipate that this distance prevents the parameters of the effective low-energy model to reach their fixed-point values which would define the relevant low-energy model just above the ground state. At present, it is unclear whether $\Delta E/L$ itself sets the cutoff scale or whether a fictitious temperature T_{quench} which induces the same excitation energy by thermal fluctuations, or yet another quantity sets the relevant scale. The fictitious temperature T_{quench} would be the most promising candidate if the system relaxed towards a thermal state on moderate time scales. But so far all numerical and analytical evidence in one-dimensional systems points against such a relaxation. In particular, there is growing evidence that integrable models such as the sine-Gordon model do no thermalize^{23–26}. Their steady-state may be characterized by a generalized Gibbs ensemble²⁸.

Mitra and Giamarchi^{14,41} argue that in interacting systems the high-energy modes act as thermal bath to the low-energy modes so that the latter behave on long time scales as if they were thermally excited. A (small) dissipation rate is computed which sets the inverse time scale for the relaxation towards this apparent thermal behavior. Though this scenario appears intuitively plausible, the studied peculiar quench in the integrable sine-Gordon model leaves the question still open how generic it is.

In view of the above arguments, one may expect three temporal regimes in one-dimensional quenched systems: (i) Short time dynamics governed by power laws with the FS exponents, (ii) Intermediate time dynamics governed by power laws with slowly varying exponents which approach the GS values, but do not reach them because their evolution is stopped by the distance of the system to its equilibrium ground state. (iii) If the systems are not integrable, the dynamics of low-energy models displays relaxation to thermal states at very long times.

Since at present, no scenario of the fascinating long time dynamics of one-dimensional systems, let alone of two- or three-dimensional systems, is firmly established further analytical and numerical work is called for. In particular, the investigation of the potential crossover regimes deserves further attention as well as the regime of very long times.

V. CONCLUSIONS

In the current work, we investigated the time evolution of the jump in the momentum distribution of two one-dimensional fermionic models after interaction quenches. The method used was the integration of the multiply iterated Heisenberg equations of motion for the opera-

tors (up to about 10^7 equations). This approach circumvents the paramount difficulty to treat quantum states of infinite systems because it focuses on the observables and their dynamics. In this dynamics, the commutation with the local Hamilton operator implies a linked-cluster property²¹ which keeps the problem finite and tractable for each finite order of powers in the time t .

The first model studied comprises spinless fermions with nearest-neighbor interaction at half-filling. For this model, a power law as found for the Tomonaga-Luttinger model provides a good description for the time evolution of the jump for short to intermediate times. The exponents can be taken from the ground state properties known from Bethe ansatz or from first order bosonization around the Fermi sea. They do not differ much as long as the quenched systems is still metallic. The excitation energy induced by the quench turns out to be remarkably small. The Fermi sea exponents fit slightly better for the quenches close to the phase transition at $U = W/2$.

The second model studied is the Hubbard model at quarter filling for which much larger excitation energies can be induced for U values of the order of the band width W . Also, the anomalous dimension K_σ in the spin channel differs significantly depending on the way it is determined, either around the Fermi sea or around the ground state. On the accessible time scales, we found that the Fermi sea parameters describe the temporal evo-

lution better than the equilibrium parameters.

We discussed possible scenarios for longer times on the basis of energy cutoffs such as the inverse time $1/t$, the excitation energy $\Delta E/L$, or a fictitious temperature T_{quench} leading thermally to the same excitation energy. The likely scenario is the occurrence of power laws with gradually changing exponents which start from the Fermi sea values and approach the equilibrium values without reaching them due to the distance of the quenched system to its equilibrium. For very long times, the low-energy modes may even show thermal relaxation if a macroscopic number of conserved quantities does not prevent it. But many further studies are called for to clarify whether this likely scenario is really the true one.

Acknowledgments

We are indebted to A. Klümper and F. Essler for help in the evaluation of the Bethe ansatz results, to V. Meden for providing data, and to F. Becca, S. Kehrein, M. Kollar, V. Meden, M. Moeckel, and J. Stolze for inspiring discussions. We acknowledge support from the Studienstiftung des deutschen Volkes (SAH), from the Mercator Stiftung in project Pr-2011-003, and from the DFG in project UH 90/5-1 (GSU).

* Electronic address: hamerla@fkt.physik.tu-dortmund.de
† Electronic address: goetz.uhrig@tu-dortmund.de

- ¹ L. Perfetti, P. A. Loukakos, M. Lisowski, U. Bovensiepen, H. Berger, S. Biermann, P. S. Cornaglia, A. Georges, and M. Wolf, Phys. Rev. Lett. **97**, 067402 (2006).
- ² M. Greiner, O. Mandel, T. Esslinger, T. W. Hänsch, and I. Bloch, Nature **415**, 39 (2002).
- ³ M. Greiner, O. Mandel, T. W. Hänsch, and I. Bloch, Nature **419**, 39 (2002).
- ⁴ P. Schmidt and H. Monien, arXiv:/0202046v1.
- ⁵ J. K. Freericks, V. M. Turkowski, and V. Zlatić, Phys. Rev. Lett. **97**, 266408 (2006).
- ⁶ M. Eckstein, M. Kollar, and P. Werner, Phys. Rev. Lett. **103**, 056403 (2009).
- ⁷ A. J. Daley, C. Kollath, U. Schollwöck, and G. Vidal, J. Stat. Mech. **2004**, P04005 (2004).
- ⁸ S. R. White and A. E. Feiguin, Phys. Rev. Lett. **93**, 076401 (2004).
- ⁹ T. Enss and J. Sirker, New J. Phys. **95**, 023008 (2012).
- ¹⁰ M. Moeckel and S. Kehrein, Phys. Rev. Lett. **100**, 175702 (2008).
- ¹¹ B. Schiró and M. Fabrizio, Phys. Rev. Lett. **105**, 076401 (2010).
- ¹² B. Sciolla and G. Biroli, J. Stat. Mech.: Theor. Exp. p. P11003 (2011).
- ¹³ A. Gambassi and P. Calabrese, Europhys. Lett. **95**, 66007 (2011).
- ¹⁴ A. Mitra and T. Giamarchi, Phys. Rev. Lett. **107**, 150602 (2011).
- ¹⁵ F. Goth and F. F. Assaad, Phys. Rev. B **85**, 085129 (2012).
- ¹⁶ A. Polkovnikov, K. Sengupta, A. Silva, and M. Vengalattore, Rev. Mod. Phys. **83**, 863 (2011), 1007.5331.
- ¹⁷ T. Barthel and U. Schollwöck, Phys. Rev. Lett. **100**, 100601 (2008).
- ¹⁸ M. A. Cazalilla, Phys. Rev. Lett. **97**, 156403 (2006).
- ¹⁹ C. Kollath, A. M. Läuchli, and E. Altman, Phys. Rev. Lett. **98**, 180601 (2007).
- ²⁰ S. R. Manmana, S. Wessel, R. M. Noack, and A. Muramatsu, Phys. Rev. Lett. **98**, 210405 (2007).
- ²¹ G. S. Uhrig, Phys. Rev. A **80**, 061602 (2009).
- ²² B. Dóra, M. Haque, and G. Zaránd, Phys. Rev. Lett. **106**, 156406 (2011).
- ²³ J. Sabio and S. Kehrein, New J. Phys. **12**, 055008 (2010).
- ²⁴ D. Fioretto and G. Mussardo, New J. Phys. **12**, 055015 (2010).
- ²⁵ A. Iucci and M. A. Cazalilla, New J. Phys. **12**, 055019 (2010).
- ²⁶ C. De Grandi, V. Gritsev, and A. Polkovnikov, Phys. Rev. B **81**, 224301 (2010).
- ²⁷ B. Sciolla and G. Biroli, Phys. Rev. Lett. **105**, 220401 (2010).
- ²⁸ M. Rigol, V. Dunjko, V. Yurovsky, and M. Olshanii, Phys. Rev. Lett. **98**, 050405 (2007).
- ²⁹ A. Luther and I. Peschel, Phys. Rev. B **12**, 3908 (1975).
- ³⁰ F. D. M. Haldane, Phys. Rev. Lett. **45**, 1358 (1980).
- ³¹ V. Meden and K. Schönhammer, Phys. Rev. B **46**, 15753 (1992).
- ³² K. Penc and J. Sólyom, Phys. Rev. B **47**, 6273 (1993).
- ³³ J. Voit, Rep. Prog. Phys. **58**, 977 (1995).
- ³⁴ E. Miranda, Braz. J. Phys. **33**, 3 (2003).

³⁵ T. Giamarchi, *Quantum Physics in One Dimension* (Clarendon Press, Oxford, 2004).

³⁶ C. Karrasch, J. Rentrop, D. Schuricht, and V. Meden, Phys. Rev. Lett. **109**, 126406 (2012).

³⁷ E. Coira, F. Becca, and A. Parola, p. 1205.2967 (2012).

³⁸ F. Pollmann, M. Haque, and B. Dóra, Phys. Rev. B **87**, 041109(R) (2013).

³⁹ A. Iucci and M. A. Cazalilla, Phys. Rev. A **80**, 063619 (2009).

⁴⁰ J. Rentrop, D. Schuricht, and V. Meden, New J. Phys. **14**, 075001 (2012).

⁴¹ A. Mitra and T. Giamarchi, Phys. Rev. B **85**, 075117 (2012).

⁴² S. A. Hamerla and G. S. Uhrig, Phys. Rev. B **87**, 064304 (2013).

⁴³ Note that version 1 of preprint 44 dealt with both subjects in a very short and not yet complete way so that we have decided to split and to extend the discussion into the present article and Ref. 42.

⁴⁴ S. A. Hamerla and G. S. Uhrig, arXiv:/1207.2006v1.

⁴⁵ E. Fradkin, *Field Theories of Condensed Matter Systems*, vol. 82 of *Lecture Annote Series* (Addison Wesley, Redwood City, 1991).

⁴⁶ C. N. Yang and C. P. Yang, Phys. Rev. **150**, 321 (1966).

⁴⁷ C. N. Yang and C. P. Yang, Phys. Rev. **150**, 327 (1966).

⁴⁸ J. Hubbard, Phys. Roy. Soc. Lond. **276**, 238 (1963).

⁴⁹ M. C. Gutzwiller, Phys. Rev. Lett. **10**, 159 (1963).

⁵⁰ J. Kanamori, Prog. Theor. Phys. **30**, 275 (1963).

⁵¹ E. H. Lieb and F. Y. Wu, Phys. Rev. Lett. **20**, 1445 (1968).

⁵² F. H. L. Essler, H. Frahm, A. Klümper, and V. E. Korepin (2005).

⁵³ P. Calabrese and J. Cardy, Phys. Rev. Lett. **96**, 136801 (2006).

⁵⁴ E. H. Lieb and D. W. Robinson, Commun. math. Phys. **28**, 251 (1972).

⁵⁵ M. Moeckel and S. Kehrein, Ann. of Phys. **324**, 2146 (2009).

⁵⁶ H. J. Schulz, Phys. Rev. Lett. **64**, 2831 (1990).

Appendix A: Convergence in the number of loops

In order to quantify the convergence properties of the approach, we study the difference of the results for the jump in momentum distribution $\Delta n_m(t)$ obtained in m loops. Taking the result with the highest number of loops (11) as reference, Fig. 7 depicts how the deviations from the 11-loop curve increase with time. Setting a certain threshold for the deviation, here 0.01, we determine up to which time t_{runaway} the deviation remains below the threshold. Fig. 7 shows data for the half filled spinless fermion case. Analogous data for the Hubbard model can be found in Ref. 42.

The choice of the threshold value is to some extent arbitrary, but it helps to illustrate the main point: The results converge for increasing number of loops $m \rightarrow \infty$.

Finally, we plot the resulting inverse runaway times in the double logarithmic plot in Fig. 8 as function of $1/m$. Clearly, the times up to which the results are reliable quickly increase on increasing loop number m . The exponent is found to be of the order of 2. Again, this is

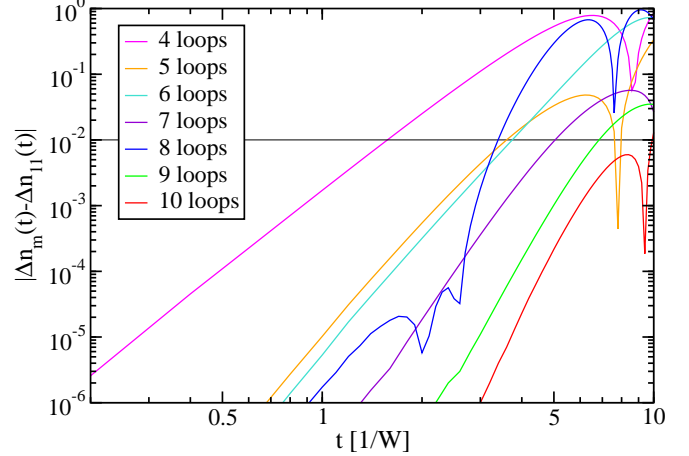


FIG. 7: (color online) Absolute difference of the jump $\Delta n_m(t)$ at various numbers of loops m relative to the 11-loop result $\Delta n_{11}(t)$ for the half filled spinless fermion model quenched by nearest-neighbor interaction. Horizontal black line: Threshold for the determination of the runaway time.

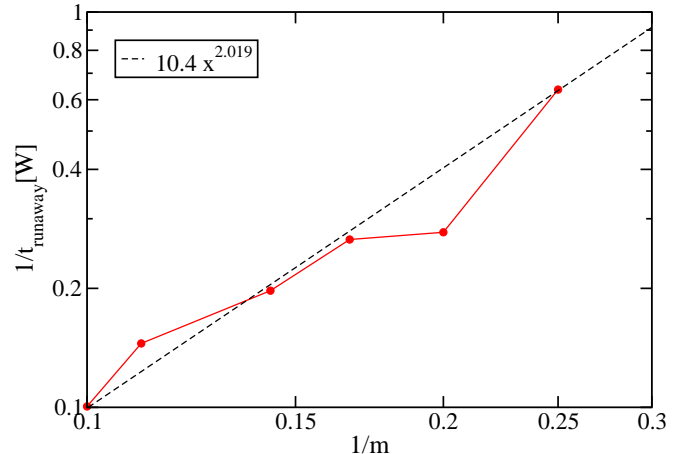


FIG. 8: (color online) Double logarithmic plot of the inverse runaway time vs. the inverse number of loops of the corresponding calculation. Dashed line: Power law fit of the data with an exponent of about 2.02.

in agreement with the previous findings for the Hubbard model⁴².